J Nanostruct 16(4): 5622-5630, Autumn 2026

RESEARCH PAPER

One-pot synthesis of Bis-spiro Piperidines Using Nanocellulose/ BF_3/Fe_3O_4 as a Natural Based Catalyst

Parisa Moharrami Korblagh [1], *Abdolhamid Bamoniri* [1]*, *Bi Bi Fatemeh Mirjalili* [2]

[1] *Department of Organic Chemistry, Faculty of Chemistry, University of Kashan, Kashan, I.R.Iran*

[2] *Department of Organic Chemistry, College of Science, Yazd University, Yazd, I.R.Iran*

ARTICLE INFO

Article History:
Received 26 May 2026
Accepted 14 September 2026
Published 01 October 2026

Keywords:
Bis-spiro piperidine
Multi-component reactions
Nanocellulose/BF_3/Fe_3O_4

ABSTRACT

Recently, multi-component reactions (MCRs) have been purposeful and they have become a serious area of research in medicinal and chemical science. A highly impressive one-pot multicomponent synthesis of bis-spiro piperidine derivatives has been reported by performing the reaction of formaldehyde, aromatic aniline and dimedone (in ratio of 3:1:2) compounds. This reaction was performed in the presence of nanocellulose/ BF_3/Fe_3O_4 as Lewis acid and heterogeneous catalyst in ethanol at room temperature. Nano-cellulose/BF_3/Fe_3O_4 as a Lewis acid catalyst has been synthesized and characterized with Field Emission Scanning Electron Microscopy (FE-SEM), Transmission Electron Microscopy (TEM), Fourier Transform Infrared (FT-IR), Thermal Gravimetry Analysis (TGA), X-ray Diffraction (XRD), X-ray fluorescence (XRF) and (Vibrating sample Magnetometry Measurements (VSM) analysis. The advantages of this protocol are low reaction time, high yield of products, simplicity of operation and reusability of catalyst. The structure of the obtained bis-spiro piperidine derivatives were studied by FT-IR and Nuclear Magnetic Resonance (^{1}H NMR) spectroscopy.

How to cite this article
Moharrami Korblagh P., Bamoniri A., Mirjalili B. One-pot synthesis of Bis-spiro Piperidines Using Nanocellulose/BF_3/Fe_3O_4 as a Natural Based Catalyst. J Nanostruct, 2026; 16(4):5622-5630. DOI: 10.22052/JNS.2026.04.092

INTRODUCTION

To produce elaborate compounds, multi-component reactions (MCRs) have been purposeful and they have become a serious area of research in medicinal chemistry [1-7]. They are defined as monovalent reactions [8] which at least three components are joined by covalent bonding [9]. Simplicity of reaction [10], single container [11], extraction and treatment hence minimize waste production12. In recent years, piperidine has been established as a significant heterocyclic compound [13-14]. The pharmacological activity of piperidine is well known [15]. Compounds containing piperidine show anticonvulsant [16], antihypertensive [17], anti-HIV [18] and anti-malarial [19] activities. Piperidines are also used as important pharmacological agents in the treatment of viral infections and diabetes [20]. Piperidines is the basic structure of many natural alkaloids [21]. Numerous methods have been reported for the preparation of spiro pipyridines. From the significance of piperidines, spiro-piperidines, which are partly lesser outstanding [22]. The prime spiro-piperidine was created by Bayer in 1900 described as a bicyclic hydrocarbon contiguous by a single carbon [23]. There has been

* *Corresponding Author Email: bamoniri@kashanu.ac.ir*

This work is licensed under the Creative Commons Attribution 4.0 International License.
To view a copy of this license, visit http://creativecommons.org/licenses/by/4.0/.

no intention to application acetic acid as a catalyst for the synthesis of spirons [24].

Recently, multitude organic reactions are synthesized using acid catalysts. The use of homogenous catalysts has received little attention [25-27]. So, the search for a cheap [28], readily available [29], and comfortable catalyst is desirable [30]. Nanoparticles are the functional component in different MCR [31], owing to the unique properties that arise from their size [32]. The catalytic activity of a catalyst is mainly resolute by its particle size. Nano-cellulose has specific importance because of its availability [33], high stability and the fact that organic groups can adjoin to its surface with strong connection [34]. Nanocellulose is an unparalleled natural polymer and biological attributes such like as biocompatibility [35-37], biodegradability and low toxicity. In this work, we apply nano-cellulose/BF_3/Fe_3O_4 as a bio-based and magnetic catalyst for the synthesis of bis-spiro substituted piperidines.

MATERIALS AND METHODS

General

The different substrates used in this study were purchased from Sigma Aldrich and Merck . TLC was carried out using silica gel G60 F254 plates (Merck). ^{1}H NMR, ^{13}C NMR spectra were recorded on a Brucker-Avance 400 MHz spectrometer using TMS as an inner standard and DMSO-d6 as a solvent. X-ray diffraction patterns were obtained with a Philips Xpert MPD diffractometer with a Cu Kα anode (k = 1.54 A˚) in the 2Θ range from 10 to 80. Field emission scanning electron microscopy was carried on a Mira 3- XMU, and transmission electron microscopy using a Philips CM120 with a LaB6 cathode and an accelerating voltage of 120 kV. X-ray fluorescence analysis was carried with a Bruker S4 Explorer instrument. Vibrating sample magnetometry measurements were carried by using a vibrating sample magnetometer.

Preparation of nano-cellulose from cotton

3 g of cotton was refluxed with 150 ml of 17.5% NaOH solution for 24 h. The obtained cotton was filtered and washed with distilled water. Then, the cotton was refluxed in solution of 15 ml of sodium hypochlorite and 55 ml of distilled water for 1.5 hours. After that, the cotton fibers were washed with distilled water. For partial acid hydrolysis and obtain nanocellulose, 60 ml of 35% sulfuric acid aqueous solution was added to cotton fibers and refluxed for 5-6 hours. The prepared suspension was diluted with water, then centrifuged at 6000 rpm.

Preparation of nanocellulose/BF_3/Fe_3O_4

0.5 ml of BF_3 was added dropwise to a mixture of nanocellulose (0.5 g) in 5 ml of dichloromethane and stirred for 20 minutes at 25 °C. Then the obtained mixture was filtered and washed with dichloromethane and dried at 25°C. After that, under ultrasound irradiation, the resulting nanocellulose/BF_3 was dispersed with 5 g of Fe_3O_4 nanoparticles in 5 ml of dichloromethane at room temperature for 1 hour. Then the resulting suspension was separated and washed with dichloromethane and dried at 25°C to obtain nanocellulose/BF_3/Fe_3O_4 catalyst.

General procedure for the synthesis of bis-spiro piperidines in the presence of nanocellulose/BF_3/Fe_3O_4 as catalyst

In a flask, a mixture of formaldehyde (3 mmol) 1,3-dicarbonyl compound (2 mmol), aniline (1 mmol), 5 mL of EtOH and 0.02 g of catalyst was mixed at room temperature for the stipulated time given in Table 2. The reaction progress was monitored by thin layer chromatography (TLC). After the completion of a reaction, the catalyst was removed from the reaction mixture by an external magnet. The solvent of reaction mixture was evaporated and the solid product was recrystallized in ethanol.

Spectroscopic data of some products

Compound 1a (Table 2, Entry 1): mp: 207-208 ºC; FTIR (KBr) ῡ: 1073, 1223, 1375, 1600-1460, 1725, 2924, 3039 cm^{-1}. ^{1}H NMR (400 MHz, $CDCl_3$, δ ppm): 7.35 (2H, d, ^3J=6.8 Hz, ArH), 7.00 (2H, d, ^3J =6.8Hz, ArH), 3.43 (4H, s, NCH_2), 2.84 (4H, d, ^2J =13.6 Hz, $COCH_2$), 2.65 (4H, d, ^2J =13.6 Hz, $COCH_2$), 2.50 (2H, s, CH_2), 1.02 (6H, s, CH_3),1.01 (6H, s, CH_3).

Compound 2a (Table 2, Entry 2) mp: 215-217 ºC; FTIR (KBr) ῡ: 767, 1229, 1389, 1593-1450, 1718, 2926, 3039 cm^{-1}. ^{1}H NMR (400 MHz, $CDCl_3$, δ ppm): 7.22 (2H, d, ^3J =8.4 Hz, ArH), 7.05 (2H, d, ^3J =8.4 Hz, ArH), 3.43 (4H, s, NCH_2), 2.85 (4H, d, ^2J =13.6 Hz, $COCH_2$), 2.66 (4H, d, ^2J =14 Hz, $COCH_2$), 2.51 (2H, s, CH_2),1.02 (12H, s, CH_3).

Compound 3a (Table 2, Entry 3) mp: 236-238 ºC; FTIR (KBr) ῡ: 1001, 1286, 1376, 1660-1493, 1749, 2955, 3050 cm^{-1}. ^{1}H NMR (400 MHz, $CDCl_3$, δ ppm): 7.30 (1H, d, ^3J =8.8 Hz, ArH), 7.13 (1H, d, ^3J =2.8 Hz, ArH), 7.02 (1H, dd, ^3J =8.8, 2.8 Hz, ArH),

CC BY

3.44 (4H, s, CH_2), 2.85 (4H, d, ^2J =14 Hz, $COCH_2$), 2.66 (4H, d, ^2J =13.6 Hz, CH_2), 2.51 (2H, s, CH_2), 1.02 (12H, s, CH_3).

Compound 4a (Table 2, Entry 4) mp: 250-253 ºC; FTIR (KBr) ū: 1248, 1380, 1610-1421, 1718, 3039, 2963 cm^{-1}. ^1H NMR (400 MHz, DMSO-d_6, δ ppm): 7.05 (2H, d, ^3J =8 Hz, ArH), 6.55 (2H, d, ^3J =8 Hz, ArH), 3.38 (4H, s, CH_2), 2.66 (3H, s, CH_3), 2.32 (4H, d, ^2J =16 Hz, CH_2), 2.10 (4H, d, ^2J =16.4 Hz, CH_2), 1.74 (2H, s, CH_2),1.05 (12H, s, CH_3).

Compound 5a (Table 2, Entry 5) mp: 188-190 ºC; FTIR (KBr) ū: 1255, 1374, 1596-1417, 1667, 2958, 3015 cm^{-1}. ^1H NMR (400 MHz, DMSO-d_6, δ ppm): 6.90 (1H, s, ArH), 6.85 (1H, d, ^3J =8 Hz, ArH), 6.64 (1H, d, ^3J =8 Hz, ArH), 6.54 (1H, t, ^3J =8.4 Hz, ArH), 2.57 (3H, s, CH_3), 3.4 (4H, s, CH_2), 2.27 (4H, d, ^2J =16.4 Hz, CH_2), 2.12 (4H, d, ^2J =16.4 Hz, CH_2), 1.75 (2H, s, CH_2), 1.04 (12H, s, CH_3).

Compound 6a (Table 2, Entry 6) mp: 188–190 ºC; FTIR (KBr) ū: 3030, 2922, 1731, 1601-1468, 1350, 1264, 1038, 1264 cm^{-1}. ^1H NMR (400 MHz, DMSO-d_6, δ ppm): 7.05 (2H, d, ^3J =6.4 Hz, ArH), 6.75 (2H, d, ^3J =7.2 Hz, ArH), 3.66 (4H, s, CH_2), 3.33 (3H, s, OCH_3), 2.23 (4H, d, 2 J =17.2 Hz, CH_2), 2.07 (4H, d, ^2J =17.2 Hz, CH_2), 1.72 (2H, s, CH_2),1.00 (12H, s, CH_3).

Compound 7a (Table 2, Entry 7) mp: 220-222 ºC; FTIR (KBr) ū: 1263, 1374, 1593, 1677-1418, 1751, 2956, 3030 cm^{-1}. ^1H NMR (400 MHz, DMSO-d_6, δ ppm): 8.03 (2H, d, ^3J =9.6 Hz, ArH), 7.22 (2H, d, ^3J =9.6 Hz, ArH), 3.83 (4H, s, NCH_2), 2.85 (4H, d, ^2J =13.6 Hz, $COCH_2$), 2.75 (4H, d, ^2J =13.6 Hz, $COCH_2$), 2.61 (2H, s, CH_2), 0.94 (6H, s, CH_3),0.92 (6H, s, CH_3).

Compound 8a (Table 2, Entry 8) mp: 186–188 ºC; FTIR (KBr) ū: 1264, 1375, 1594, 1677-1449, 1751, 2956, 3030 cm^{-1}. ^1H NMR (400 MHz, $CDCl_3$, δ ppm): 7.75 (1H, dd, ^3J =8.2, 2.0, ArH), 7.59 (1H, dd, ^3J =8.2, 2.0 Hz, ArH), 7.42 (1H, t, ^3J =8.0 Hz, ArH), 3.57 (4H, s, NCH_2), 2.87 (4H, d, ^2J =14.0 Hz, $COCH_2$), 2.69 (4H, d, ^2J =14.0 Hz, $COCH_2$), 2.56 (2H, s, CH_2), 1.04 (6H, s, CH_3), 1.03 (6H, s, CH_3).

Compound 9a (Table 2, Entry 9) mp: 140–142 ºC; FTIR (KBr) ū: 1094, 1238, 1381, 1598-1469, 1698, 2924 cm^{-1}. ^1H NMR (400 MHz, DMSO-d_6, δ ppm): 7.28-7.37 (4H, m, ArH), 3.35 (4H, s, NCH_2), 2.82 (4H, s, $COCH_2$), 2.73 (4H, s, $COCH_2$), 2.04 (2H, s, CH_2), 1.00 (6H, s, CH_3),0.96 (6H, s, CH_3).

Compound 10a (Table 2, Entry 10) mp: 189–191 ºC; FTIR (KBr) ū: 1264, 1375, 1594, 1677-1449, 1751, 2956, 3030 cm^{-1}. ^1H NMR (400 MHz, $CDCl_3$, δ ppm): 7.86 (1H, s, ArH), 7.59 (1H, t, ^3J =8.0 Hz, ArH), 7.48 (1H, t, ^3J =8.0 Hz, ArH), 3.62 (4H, s, NCH_2), 2.87 (4H, d, ^2J =14.0 Hz, $COCH_2$), 2.69 (4H, d, ^2J =14.0 Hz, $COCH_2$), 2.59 (2H, s, CH_2), 0.96 (12H, s, CH_3).

Compound 11a (Table 2, Entry 11) mp: 189–191 ºC; FTIR (KBr) ū: 1264, 1375, 1594, 1677-1449, 1751, 2956, 3030 cm^{-1}. ^1H NMR (400 MHz, $CDCl_3$, δ

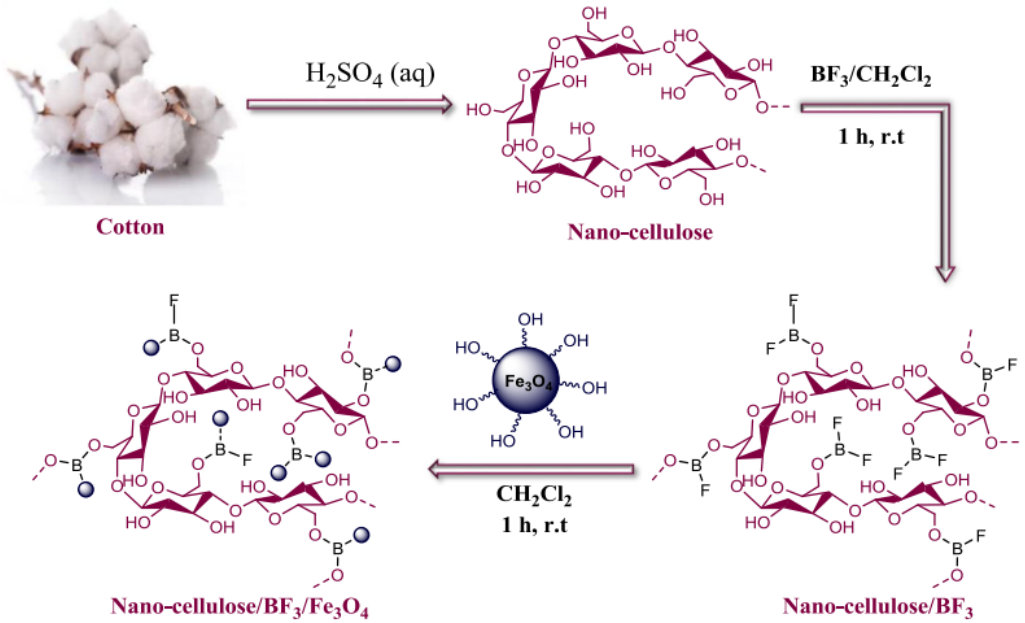


Fig. 1. Preparation of nano-cellulose/BF_3/Fe_3O_4.

CC BY

ppm): 8.86 (1H, s, OH), 7.86 (1H, d, ArH), 7.59 (1H, d, ^3J =8.0 Hz, ArH), 7.48 (2H, t, ^3J =8.0 Hz, ArH), 3.62 (4H, s, NCH_2), 2.87 (4H, d, ^2J =14.0 Hz, $COCH_2$), 2.69 (4H, d, 2 J =14.0 Hz, $COCH_2$), 2.59 (2H, s, CH_2), 0.96 (12H, s, CH_3).

Compound 12a (Table 2, Entry 12) mp: 208-209 ºC; FTIR (KBr) ῡ: 1073, 1223, 1375, 1600-1460, 1725, 2924, 3039 cm^{-1}. ^1H NMR (400 MHz, DMSO, δ ppm) 7.05 (d, J = 8.2 Hz, 1H), 7.00 (s, 1H), 3.35 (s, 2H), 2.82 (s, 2H), 2.72 (d, J = 13.5 Hz, 2H), 0.94 (s, 3H), 0.91 (s, 6H).

RESULTS AND DISCUSSION

Nanocellulose was prepared by partial hydrolysis of cellulose in cotton. Nanocellulose/BF_3 was preparate via reaction of $BF_3.OEt_2$ with nanocellulose in CH_2Cl_2. For magnetization of nanocellulose/BF_3, the synthesized Fe_3O_4 was mixed with nanocellulose/BF_3 in CH_2Cl_2 under ultrasonic condition. In result, nanocellulose/BF_3/Fe_3O_4 was obtained as a magnetic brown powder (Fig. 1).

Identification and investigation of nano cellulose/BF_3/Fe_3O_4 structure was done using various methods such as FT-IR, FESEM, XRF, XRD, TGA, VSM, and TEM. The FT-IR spectrum of nano-cellulose shows the stretching vibrations of the OH group at 3339 cm^{-1} and the stretching vibrations

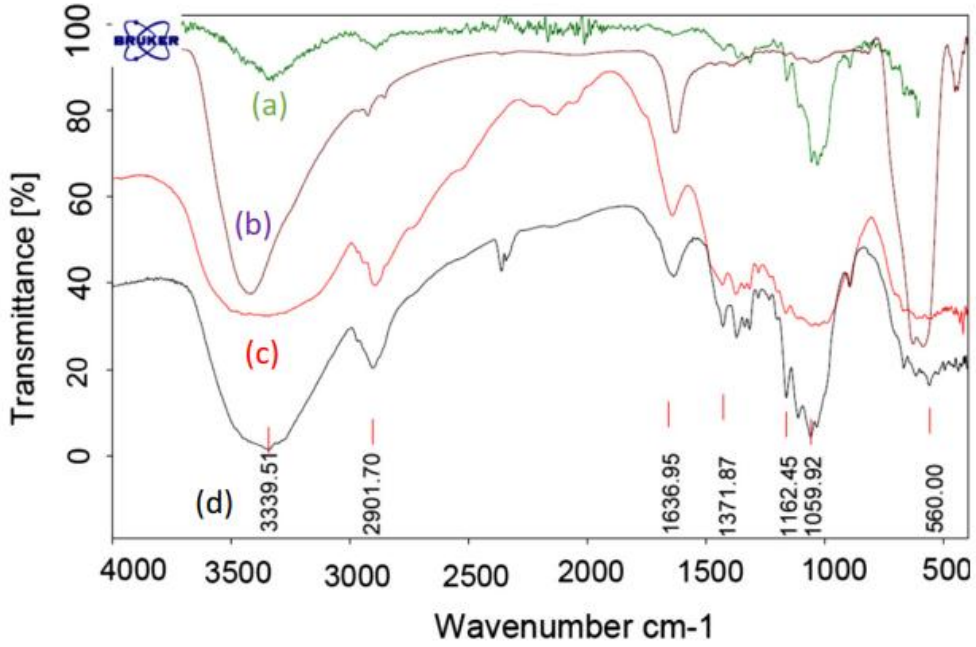


Fig. 2. FT-IR spectra of a) nano-cellulose, b) Fe_3O_4, c) nanocellulose/BF_3/Fe_3O_4 and d) recovered nanocellulose/BF_3/Fe_3O_4.

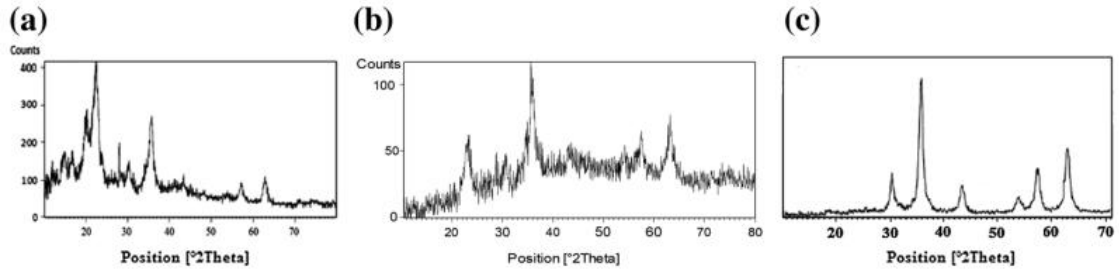


Fig. 3. XRD patterns of the a) fresh nanocellulose/BF_3/Fe_3O_4, b) reused nanocellulose/BF_3/Fe_3O_4 and c) Fe_3O_4.

CC BY

of the C–O group at around 1059 and 1162 cm^{-1}. In the FT-IR spectrum of nano-cellulose/BF_3/Fe_3O_4, in addition to the above-mentioned bands, the stretching vibrations of the Fe/O bond appears at 560 cm^{-1}. The band at 1371 cm^{-1} displays the stretching vibrations of the B–O bond, indicating

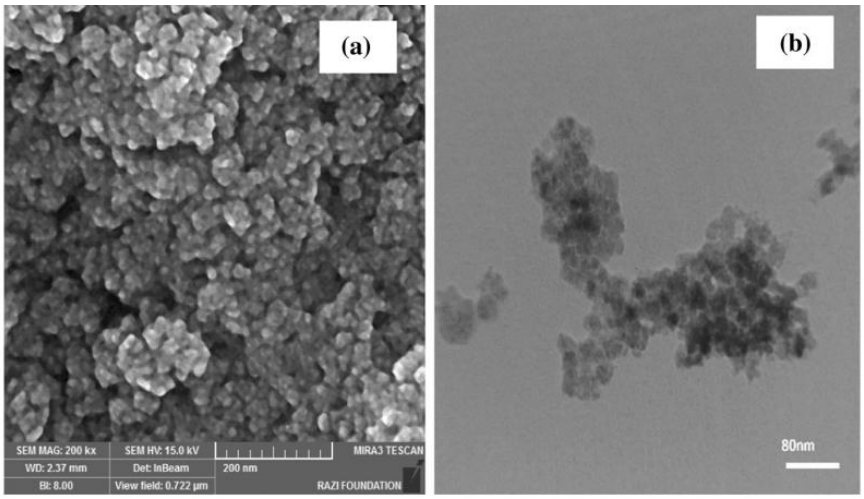


Fig. 4. a) FESEM image of nanocellulose/BF_3/Fe_3O_4, b) TEM image of nanocellulose/BF_3/Fe_3O_4.

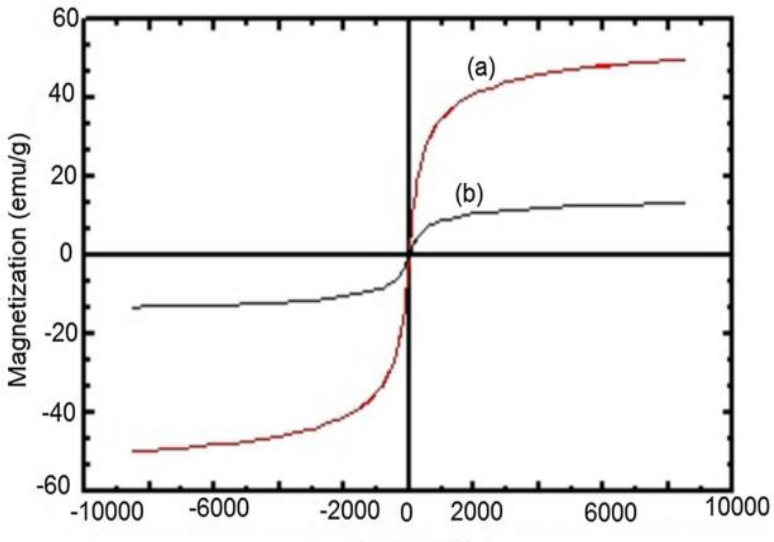


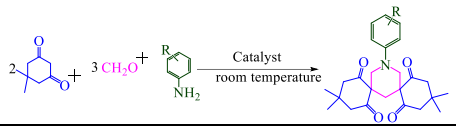
Fig. 5. Magnetization loops of a) Fe_3O_4 and b) nanocellulose/BF_3/Fe_3O_4.

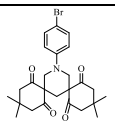
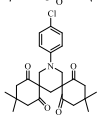
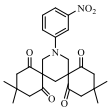
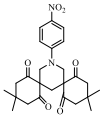
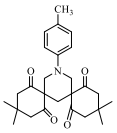
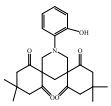
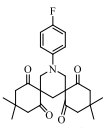
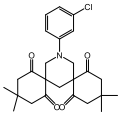
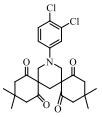
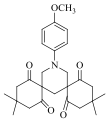
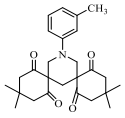
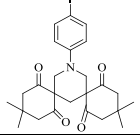
Table 1. Results of XRF analysis of catalyst and standard samples of H_3BO_3 and NaF.

Elemental Component	Nano-cellulose/BF_3/Fe_3O_4			NH_3BO_3		NaF	
	B%	F%	KCPS	B%	KCPS	F%	KCPS
B	3.496	-	0.5	17.48	2.5	-	
F	-	1.112	1	-		45.25	40.7

CC BY

Table 2. Synthesis of bis-spiro piperidines in the presence of nanocellulose/BF_3/Fe_3O_4 as catalyst.



Entry	Product	Mp (C)	Structure	yeld (%)	time (min)
1	1a	202–204		93%	20
2	2a	204–206		92%	21
3	3a	213–214		91%	30
4	4a	217–219		89%	36
5	5a	189–192		86%	39
6	6a	197–200		83%	43
7	7a	219–222		82%	44
8	8a	190–194		80%	48
9	9a	190–194		78%	49
10	10a	190–194		75%	50
11	11a	190–194		74%	54
12	12a	208-209		75%	60

[a] Reaction conditions: dimedone (2.0 mmol), Formaldehyde (3.0 mmol) and aniline (1.0 mmol) in the presence of nano-cellulose/BF_3/Fe_3O_4 in EtOH under room temperature conditions, [b] Isolated yield

CC BY

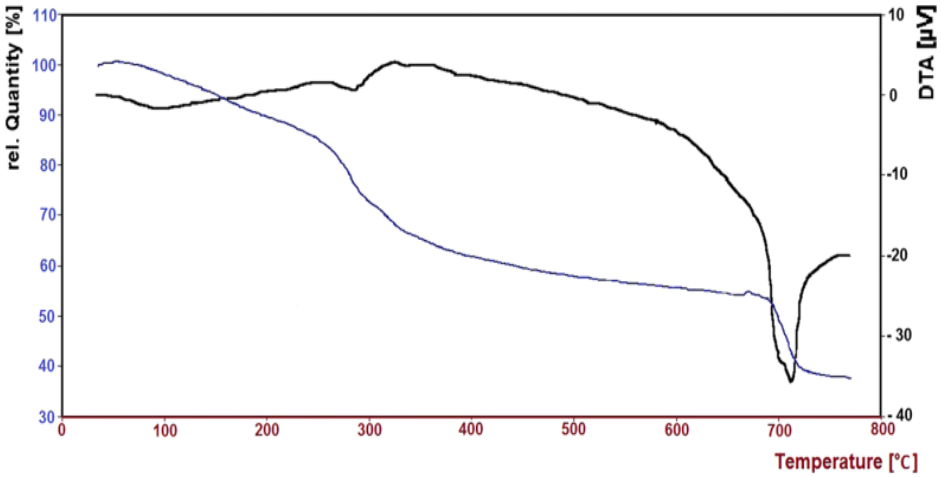


Fig. 6. Thermal gravimetric analysis pattern of nanocellulose/BF_3/Fe_3O_4.

that the BF_3 is supported on the nano-cellulose (Fig. 2).

XRD diagrams of fresh nanocellulose /BF_3/Fe_3O_4, reused nanocellulose /BF_3/Fe_3O_4 and Fe_3O_4 are shown in Fig. 3. According to the XRD diagram of nano-cellulose /BF_3/Fe_3O_4 (Fig. 3a), the signals in 2Θ equal to 23 and 13 are attributed to cellulose section of catalyst. The signals 2Θ = 30, 35.5, 43, 53.5, 57 and 62.9 indicate the presence of Fe_3O_4.

The shape and size of nanocellulose/BF_3/Fe_3O_4 nanoparticles were investigated and evaluated using FESEM and TEM (Fig. 4). The images show that the nanoparticles of nanocellulose /BF_3/Fe_3O_4 are on average about 22 nm.

X-ray fluorescence (XRF) method was used for elemental analysis of nanocellulose/BF_3/Fe_3O_4. To determine the boron: fluorine ratio in the catalyst, the number of kilograms per second of the elements in the catalyst was evaluated with KCPS of the elements in high-purity H_3BO_3 and NaF (Table 1). The calculated values for boron and fluoride are 3.496 mol and 0.059 mol, respectively. Therefore, the boron:fluorine ratio in the catalyst is approximately 5:1.

The magnetic properties of Fe_3O_4 and nanocellulose/BF_3/Fe_3O_4 at 300 K were detected using vibrating sample magnetometer (VSM) technique (Fig. 5). According to the residual ring magnetization, there is no residual magnetization and also the coercivity value is zero for both samples, which proves the superparamagnetic property of the samples in room. The findings prove that the binding of cellulose to nanocellulose/BF_3/Fe_3O_4 decreases the saturation magnetization. Despite of this reduction, the catalyst can still be easily separated from the reaction medium using an external magnetic.

Thermogravimetric analysis (TGA) of nanocellulose/BF_3/Fe_3O_4 was done in the temperature range of 35 °C to 770 °C (Fig. 6). The TGA chart of catalyst shows three parts of weight loss. The first weight loss (6%) in range of 95 °C to 150 °C is related to the removal of moisture from the catalyst. The second weight loss (33%) is the range of 263-336 °C is related to the decomposition of cellulose section of catalyst. The char yield of catalyst in 700 °C is 40%.

After identification of the structure properties of nanocellulose/BF_3/Fe_3O_4, we have applied this catalyst for synthesis of bis-spiro piperidine derivatives. The best condition for this synthesis is using dimedone (2 mmol), formaldehyde (3 mmol), aniline derivative (1 mmol), ethanol (5 ml) and catalyst (0.02 g) at room temperature. The synthesized derivatives of bis-spiro piperidine are tabulated in Table 2.

CONCLUSION

In this study, a nanocellulose/BF_3/Fe_3O_4 composite was prepared and applied as a magnetically separable catalyst for the one-pot synthesis of bis-spiro piperidine derivatives. Characterization by FT-IR, XRD, FESEM, TEM, XRF, VSM, and TGA supported the formation of the composite, with an average particle size of approximately 22 nm

CC BY

and superparamagnetic behavior at room temperature. The multicomponent reaction of dimedone, formaldehyde, and aniline derivatives was conducted in ethanol at room temperature using 0.02 g of the catalyst. The combination of a renewable nanocellulose support, ambient-temperature conditions, and straightforward magnetic separation offers practical advantages for preparing these heterocyclic compounds. Further investigations into catalyst recyclability, component leaching, and substrate scope would help establish the long-term performance and broader applicability of this catalytic system.

ACKNOWLEDGEMENT

The authors are grateful to University of Kashan for financial support of this work.

CONFLICT OF INTEREST

The authors declare that there is no conflict of interests regarding the publication of this manuscript.

REFERENCES

1. Reddy BM, Sreekanth PM, Lakshmanan P. Sulfated zirconia as an efficient catalyst for organic synthesis and transformation reactions. J Mol Catal A: Chem. 2005;237(1-2):93-100.
2. Clark JH. Solid Acids for Green Chemistry. Acc Chem Res. 2002;35(9):791-797.
3. Alinezhad H, Tajbakhsh M, Zare M. Catalyst-free one-pot synthesis of 1,4,5-trisubstituted pyrazoles in 2,2,2-trifluoroethanol. Journal of Fluorine Chemistry. 2011;132(11):995-1000.
4. Daryabari M, Khaksar S. Green synthesis of highly substituted pyridines via the one-pot multi-component reaction in 2,2,2-trifluoroethanol. J Mol Liq. 2014;198:263-266.
5. Rostamnia S, Doustkhah E. A mesoporous silica/fluorinated alcohol adduct: an efficient metal-free, three-component synthesis of indazolophthalazinetrione heterocycles using a reusable nanoporous/trifluoroethanol adduct (SBA-15/TFE). Tetrahedron Lett. 2014;55(15):2508-2512.
6. De K, Legros J, Crousse B, Bonnet-Delpon Dl. Solvent-Promoted and -Controlled Aza-Michael Reaction with Aromatic Amines. The Journal of Organic Chemistry. 2009;74(16):6260-6265.
7. Rashmi SV, Sandhya NC, Raghava B, Kumara MN, Mantelingu K, Rangappa KS. Trifluoroethanol as a Metal-Free, Homogeneous, and Recyclable Medium for the Efficient One-Pot Synthesis of Dihydropyrimidones. Synth Commun. 2011;42(3):424-433.
8. Doustkhah E, Rostamnia S, Hassankhani A. The raise of SBA-SO_3H catalytic activity by inducing ultrasound irradiation in the multicomponent syntheses. J Porous Mater. 2015;23(2):549-556.
9. Rostamnia S, Doustkhah E. Increased SBA-15-SO_3H Catalytic Activity through Hydrophilic/Hydrophobic Fluoroalkyl-Chained Alcohols (RFOH/SBA-15–Pr-SO_3H). Synlett. 2015;26(10):1345-1347.
10. Rostamnia S, Doustkhah E, Nuri A. Hexafluoroisopropanol dispersed into the nanoporous SBA-15 (HFIP/SBA-15) as a rapid, metal-free, highly reusable and suitable combined catalyst for domino cyclization process in chemoselective preparation of alkyl rhodanines. Journal of Fluorine Chemistry. 2013;153:1-6.
11. Rostamnia S, Doustkhah E, Bahrami K, Amini S. An increase in the cooperative catalytic performance of SBA-15 and TFE in selective oxidation of organic sulfides. J Mol Liq. 2015;207:334-337.
12. Rostamnia S, Zabardasti A. SBA-15/TFE (SBA-15/2,2,2-trifluoroethanol) as a suitable and effective metal-free catalyst for the preparation of the tri- and tetra-substituted imidazoles via one-pot multicomponent method. Journal of Fluorine Chemistry. 2012;144:69-72.
13. Shuklov I, Börner A, Dubrovina N. Fluorinated Alcohols as Solvents, Cosolvents and Additives in Homogeneous Catalysis. Synthesis. 2007;2007(19):2925-2943.
14. Cioc RC, Ruijter E, Orru RVA. Multicomponent reactions: advanced tools for sustainable organic synthesis. Green Chem. 2014;16(6):2958-2975.
15. Xin X, Wang Y, Kumar S, Liu X, Lin Y, Dong D. Efficient one-pot synthesis of substituted pyridines through multicomponent reaction. Organic and Biomolecular Chemistry. 2010;8(13):3078.
16. Jadhav AM, Balwe SG, Lim KT, Jeong YT. A novel three-component method for the synthesis of spiro[chromeno [4′,3′:4,5] pyrimido[1,2- b] indazole-7,3′-indoline]-2′,6(9 H)-dione. Tetrahedron. 2017;73(19):2806-2813.
17. Ghahremanzadeh R, Imani Shakibaei G, Ahadi S, Bazgir A. One-Pot, Pseudo Four-Component Synthesis of a Spiro[diindeno[1,2-b:2′,1′-e]pyridine-11,3′-indoline]-trione Library. J Comb Chem. 2009;12(1):191-194.
18. Li J, Wu N, Tian Y, Zhang J, Wu S. Aminopyridyl/Pyrazinyl Spiro[indoline-3,4′-piperidine]-2-ones As Highly Selective and Efficacious c-Met/ALK Inhibitors. ACS Med Chem Lett. 2013;4(8):806-810.
19. Kozlov NG, Kadutskii AP. A novel three-component reaction of anilines, formaldehyde and dimedone: simple synthesis of spirosubstituted piperidines. Tetrahedron Lett. 2008;49(29-30):4560-4562.
20. Ye L, Tian Y, Li Z, Jin H, Zhu Z, Wan S, et al. Design, synthesis and molecular docking studies of some novel spiro[indoline-3, 4′-piperidine]-2-ones as potential c-Met inhibitors. Eur J Med Chem. 2012;50:370-375.
21. Padvi SA, Tayade YA, Wagh YB, Dalal DS. [bmim]OH: An efficient catalyst for the synthesis of mono and bis spirooxindole derivatives in ethanol at room temperature. Chin Chem Lett. 2016;27(5):714-720.
22. Viegas C, da S. Bolzani V, Furlan M, Barreiro EJ, Young MCM, Tomazela D, et al. Further Bioactive Piperidine Alkaloids from the Flowers and Green Fruits of Cassia spectabilis. J Nat Prod. 2004;67(5):908-910.
23. Ho B, Michael Crider A, Stables JP. Synthesis and structure–activity relationships of potential anticonvulsants based on 2-piperidinecarboxylic acid and related pharmacophores. Eur J Med Chem. 2001;36(3):265-286.
24. Kumar RR, Perumal S, Senthilkumar P, Yogeeswari P, Sriram D. Discovery of Antimycobacterial Spiro-piperidin-4-ones: An Atom Economic, Stereoselective Synthesis, and Biological Intervention. J Med Chem. 2008;51(18):5731-5735.
25. Misra M, Pandey SK, Pandey VP, Pandey J, Tripathi R, Tripathi RP. Organocatalyzed highly atom economic one pot synthesis of tetrahydropyridines as antimalarials. Bioorganic and Medicinal Chemistry. 2009;17(2):625-633.

CC BY

26. Weis R, Schweiger K, Faist J, Rajkovic E, Kungl AJ, Fabian WMF, et al. Antimycobacterial and H1-antihistaminic activity of 2-substituted piperidine derivatives. Bioorganic and Medicinal Chemistry. 2008;16(24):10326-10331.
27. Petit S, Nallet JP, Guillard M, Dreux J, Chermat R, Poncelet M, et al. Synthèses et activités psychotropes de 3,4-diarylpipéridines. Corrélation structure-activité et recherche d'une activité antihypertensive. Eur J Med Chem. 1991;26(1):19-32.
28. Zhou Y, Gregor VE, Ayida BK, Winters GC, Sun Z, Murphy D, et al. Synthesis and SAR of 3,5-diamino-piperidine derivatives: Novel antibacterial translation inhibitors as aminoglycoside mimetics. Bioorganic and Medicinal Chemistry Letters. 2007;17(5):1206-1210.
29. Mukhopadhyay C, Rana S, Butcher RJ. FeCl3 catalysed two consecutive aminomethylation at the α-position of the β-dicarbonyl compounds: an easy access to hexahydropyrimidines and its spiro analogues. Tetrahedron Lett. 2011;52(32):4153-4157.
30. Dandia A, Jain AK, Sharma S. Indium triflate catalyzed one-pot multicomponent synthesis of spiro-hexahydropyrimidines explained by multiple covalent bond formation. Tetrahedron Lett. 2012;53(39):5270-5274.
31. Atar AB, Jeong YT. Silica supported tungstic acid (STA): an efficient catalyst for the synthesis of bis-spiro piperidine derivatives under milder condition. Tetrahedron Lett. 2013;54(10):1302-1306.
32. Ray S, Bhaumik A, Banerjee B, Manna P, Mukhopadhyay C. Heterogeneous silica-supported copper catalyst for the ultrasound-mediated rapid reaction between dimedone, formaldehyde, and amines at room temperature. Monatshefte für Chemie - Chemical Monthly. 2015;146(11):1881-1890.
33. Sahu PK, Sahu PK, Agarwal DD. Efficient and facile synthesis of heterocycles and their mechanistic consideration using kaolin. RSC Advances. 2013;3(25):9854.
34. Sahu PK, Sahu PK, Sharma Y, Agarwal DD. Synthesis and Mechanistic Study of Triheterocyclic 4H-Pyrimido[2,1-b] benzothiazole derivatives, One-Pot Three-component Reaction under Solvent-Free Conditions. J Heterocycl Chem. 2014;51(4):1193-1198.
35. Azad S, Fatameh Mirjalili BB. Fe_3O_4 @nano-cellulose/TiCl: a bio-based and magnetically recoverable nano-catalyst for the synthesis of pyrimido[2,1-b]benzothiazole derivatives. RSC Advances. 2016;6(99):96928-96934.
36. Azad S, Mirjalili BBF. Nano-$TiCl_2$/cellulose: an eco-friendly bio-based catalyst for one-pot synthesis of 4H-pyrimido[2,1-b]benzothiazole derivatives. Res Chem Intermed. 2016;43(3):1723-1734.
37. Atar AB, Jeong YT. FeF_3 catalyzed cascade C–C and C–N bond formation: synthesis of differentially substituted triheterocyclic benzothiazole functionalities under solvent-free condition. Mol Divers. 2014;18(2):389-401.

CC BY